ESTIMATION OF SUBSURFACE STRUCTURE BASED ON MICROTREMOR, BORE HOLE OBSERVATIONS AND STOCHASTIC STRONG GROUND MOTION SIMULATIONS IN PALU CITY, CENTRAL SULAWESI, INDONESIA: A VALIDATION AND SENSITIVITY STUDY ON THE 23 JANUARY 2005 (PALU) EARTHQUAKE

Pyi Soe Thein[*1], Subagyo Pramumijoyo[2], Wahyu Wilopo[2], Agung Setianto[2], Kirbani Sri Brotopuspito[3], and Junji Kiyono[4]

[1]*Geology Department, Yadanabon University, Mandalay, Myanmar*
[2]*Geological Engineering Department, Favulty of Engineering, Gadjah Mada University, Yogyakarta, Indonesia*
[3]*Physics Department, Gadjah Mada University, Yogyakarta, Indonesia*
[4]*Graduate School of Global Environmental Studies, Kyoto University, Kyoto, Japan*

Abstract

In this study, we investigated the subsurface structure and strong ground motion parameters for Palu City. One of the major structures in Central Sulawesi is the Palu-Koro Fault system. Several powerful earthquakes have struck along the Palu-Koro Fault during recent years, one of the largest of which was an M 6.3 event that occurred on January 23, 2005 and caused several casualties. Following the event, we conducted a microtremor survey to estimate the shaking intensity distribution during the earthquake. From this survey we produced a map of the peak ground acceleration, velocity and ground shear strain in Palu City. We performed single observations of microtremors at 151 sites in Palu City. The results enabled us to estimate the site-dependent shaking characteristics of earthquake ground motion. We also conducted 8-site microtremor array investigation to gain a representative determination of the soil condition of subsurface structures in Palu.

From the dispersion curve of array observations, the central business district of Palu corresponds to relatively soil condition with Vs $\leq$ 300 m/s, the predominant periods due to horizontal vertical ratios (HVSRs) are in the range of 0.4 to 1.8 s and the resonant frequency are in the range of 0.7 to 3.3 Hz. Three boreholes were throughout the basin especially in Palu area to evaluate the geotechnical properties of subsurface soil layers. The depths are varying from 1 m to 30 m. Strong ground motions of the Palu area were predicted based on the empirical stochastic green's function method. Peak ground acceleration and peak ground velocity becomes more than 0.04 g and 30 kine in some areas, which causes severe damage for buildings in high probability.
Keywords: *Palu-Koro fault, microtremor, bore holes, peak ground acceleration and velocity.*

1 Introduction

Sulawesi Island, eastern Indonesia, is located at the junction between the converging Pacific-Philippine, Indo-Australian Plates and the Sundaland, i.e., the south-eastern part of the

---

*Corresponding author: P.S. THEIN, Geology Department, Yadanabon University, Mandalay, Myanmar. E-mail: pyisoethein@yahoo.com
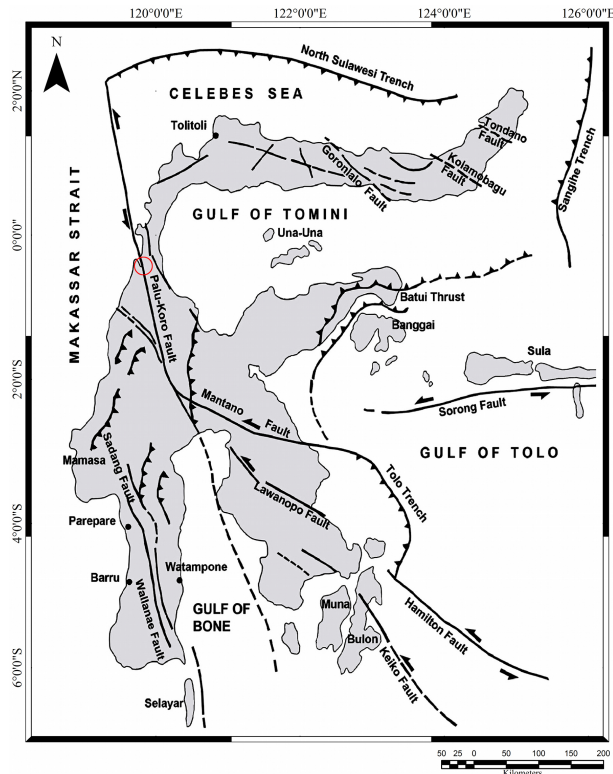
Figure 1: Tectonic map of Sulawesi, (Priadi, 1993). Red circle: Palu depression area.

Eurasian Plate. The Central Sulawesi Fault System, one of the major structures in SE Asia, cuts across Sulawesi Island from NW to SE, connecting the North Sulawesi subduction zone to the Banda Sea deformation zones. One of the major structures in Central Sulawesi is the Palu-Koro Fault system, which extends NNW- SSE direction and cross cuts Sulawesi along more than 300 km, from the North Sulawesi trench pass through Palu Bay, southward turn to the SE connect to the Matano and Lawanopo Faults and further eastward, both faults join to Tolo trench, (Priadi, 1993) (Figure 1). In this study, Palu, where a large earthquake is expected in the near future, is considered to be a target area (Thein *et al.*, 2013).

We carried out higher density single point observations and larger radius array observations. Based on the observed data, we calculated the distribution of the predominant, depth of the engineering bed rock and phase velocities of the Rayleigh wave in Palu City.

2 Seismicity

Seismicity of Palu was reported since 19th century. Location of epicenters and level of intensity were still approximate based on the European resident note. Earthquake is one of the most devastating natural phenomena. The most important earthquakes that stroke Palu, are in 1927. These earthquakes caused 2,500 people died and 750 houses were severely damaged. These data show that Palu depression area is very vulnerable to earthquake disasters (USGS, 2007).

1. December 1, 1927 earthquake, this earthquake originated at -0.7° S and 119.7° E with the magnitude of 6.3. It shocked West Central Sulawesi, Palu City area, resulted in 15 m height tsunami occurred, 14 killed, 30 injured and 0.5 to 12 m subsidence.

2. March 7, 1960 earthquake, it occurred at -1.5° N and 125.5° E with moderate intensities in regional scale with the magnitude of 5.1 and the depth of 60 km.

3. April 11, 1967 earthquake, this earthquake occurred at -3.3° S and 119.4° E with the magnitude of 6.3 and thrust fault mechanism. Tinambung area felt maximum intensity of VIII –VIII, resulted in 58 killed, 100 injured and the water suddenly retreated.

4. August 14, 1968 earthquake, it originated at -0.7° N and 118.8° E with high intensities magnitude of 7.4 and normal fault mechanism. West Central Sulawesi, Palu bay felt maximum intensity of VIII –VIII, resulted in 10 m height tsunami occurred, 200 died, 2-3 m subsidence in Mapaga village and 2-3 m subsidence.

5. February 2, 1969 earthquake, this earthquake happened at the epicenter of -3.1° S and 118.5° E with the magnitude of 6. South Sulawesi, Majene area felt maximum intensities of VIII with thrust fault mechanism, resulted in 2 to 6 m height tsunami occurred, 64 killed and over 1,200 buildings were wrecked. Eighty percent of the brick structures were damaged, and some completely collapsed. Ground fissures were noted in several places. Several

wooden houses located at the end of a bay were swept away by the waves. The press reported that the tsunami took 600 lives.

6. March 3, 1977 earthquake, this earthquake occurred at -1.99° N and 123.05° E with the magnitude of 5.4 and the depth of 58 km.

7. January 8, 1984 earthquake, this earthquake occurred at -2.77° S and 118.8° E with the magnitude of 6.6. The maximum intensity of the earthquake was VII in Mamuju area with thrust fault mechanism.

8. January 1, 1996 earthquake, this earthquake happened at -0.83° N and 120.1° E with moderate and high intensities in regional scale with the magnitude of 7.7. It shocked West coast Central Sulawesi area, resulted in 1.0 to 3.4 tsunami height occurred, 0.5 to 2.0 m subsidence, 9 killed and 63 injured.

9. January 23, 2005 earthquake, this earthquake occurred at -1.198° S and 119.933° E with the magnitude of 6.3 and the depth of 20 km in Sulawesi.

10. August 30, 2011 earthquake, this earthquake occurred at 6.401° S and 126.774° E with the magnitude of 6.8 and the depth of 465 km.

11. August 18, 2012 earthquake, this earthquake happened at -1.21° S and 120.08° E with the magnitude of 6.2 and the depth of 40 km. In Kulawi, Palu City, resulted in heavy damaged buildings.

3 Geology

Evolution of Neogene kinematics along the Palu-Koro fault was confirmed based on microtectonics approach, i.e., sinistral strike-slip due to E-W compression, radial extensions caused by telescoping vertical movement of Neogene granitoid, and then left lateral with normal component displacement due to N-S extension/ E-W compression which is still active actually (Pramumijoyo *et al.*, 1997). Palu depression area is filled by mostly clay, silt, and sand deposits as alluvial deposits, except on the border east or west consist of gravelly sands as colluvial wedges. The composition of gravel is granitic fragment to the northwest, mostly of
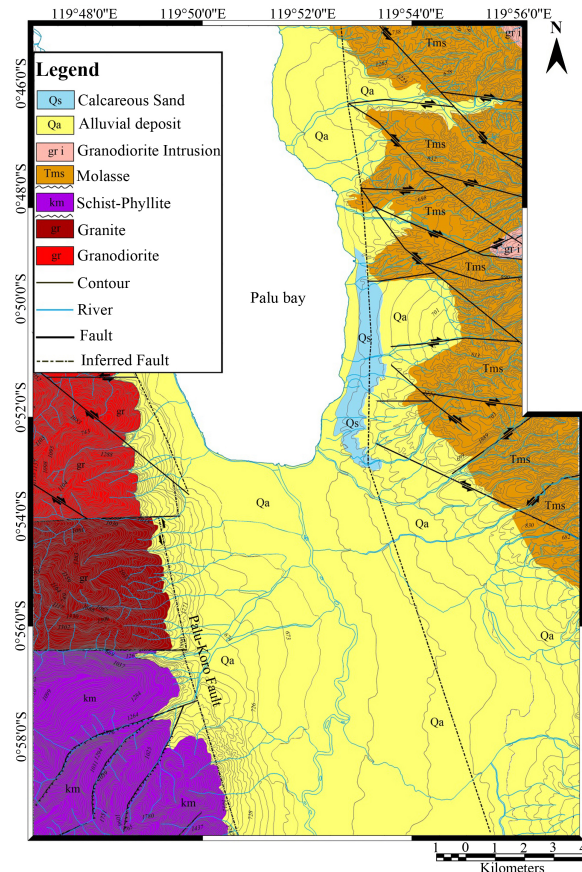

Figure 2: Geological map of Palu depression area (Ananda, 2013; Indra, 2013; Ismawan, 2013; and Juwanto, 2013).

schist on the west and to the east the gravel consists of schist, igneous and sedimentary rocks. West escarpment to the north consists of granite and granodiorite units, and to the south consists of schist-phyllitic units. East escarpment consists of molasses (Soekamto, 1995). Figure 2 shows geological map of Palu depression area.

4 The GIS based model proposed for seismic microzonation

The GIS based model that can be used to create the infrastructure of seismic microzonation studies on Palu City that have a risk in terms of natural disaster, particularly earthquake. In addition, a relational database was designed to cope with the damage resulting from natural hazards for this study.This model was applied so as to take the measures needed for the City of Palu located on the segments of the Palu-Koro

Fault Zone, a settlement with earthquake risk on the natural disaster. During creation of the system, geological, geotechnical data and data produced from aerial photos were integrated and assessed on a GIS environment. The infrastructure for seismic microzonation was created using this model. The potential areas for strong ground motion were detected in the study area. Thus, the future results were produced to assist in seismic microzonation.

5 Microtremor single station observations

A three-component accelerometer with data logger, GPL-6A3P, produced by the Mitsutoyo Co. Ltd., was used. The number of single point observations was 151 (Figure 3a). The sampling frequencies were 100 Hz or 500 Hz and the observation times were 10 to 15 minutes. This exploration method was established after the pioneering work done by Aki (1957). Although there are 151 observation points, the points are not adequate to cover all the target area. If each value of the predominant period obtained is considered to be a realization of a stochastic random field. Space interpolation is conducted by ordinary kriging technique (Kiyono *et al.*, 1996). The results are shown in Figure 3b. The predominant periods of 1.0–1.8 seconds were on the alluvial fan area. The spatial correlations between predominant periods on the west side mountain, of which slope is steep, are shorter than those in the east side mountain and change more rapidly.

6 Microtremor array observations

We carried out array observations at eight sites in Palu (Figure 3c). Four accelerometers were used in each array observation site. One was installed at a center of the circle with a radius (r). Other three were arranged on the circle with a shape of regular triangle. Observation duration time was 20~30 minutes and sampling frequency was 100Hz. Sequential observations were conducted three times by changing the array radius; r = 3, 10 and 30 meters. Dispersion curves were calculated using the SPAC method. The velocity of surface wave is well known to vary as a function of frequency (or period) due to dispersive characteristics. Therefore, the subsurface structure can be estimated from observed dispersion curve. Then, a substructure profile was identified from the dispersion curve by using the Particle Swarm Optimization (Keneddy, 1995; Noguchi *et al.*, 2009).

The dispersion curves obtained are shown in Figure 4a–c for each survey. For line A, the phase velocity corresponding to shallow ground with a high frequency range is about 369 m/s at APP, about 423 m/s at GWL, about 318 m/s at KDM, about 318 m/s at KRP, about 279 m/s at LSS, about 348 m/s at MOP, about 285 m/s at MSQ and about 317 m/s at SGI. The soft ground extended beneath LSS, which is the nearest site to the coast. The ground beneath the sites higher than GWL has relatively hard surface soil compared with the plain along the coast. Since the minimum phase velocity in the high frequency range is around 300 m/s, the soil profile is very similar along line B and line C. The dispersion curves obtained here had no discrepancies in the distribution of topography, altitude and predominant period. We could estimate subsurface sedimentary layers in the plains using these dispersion curves.

7 Estimations vs structure and inversion

7.1 Application of PSO

By conducting an inversion analysis using the Particle Swarm Optimization (PSO) algorithm on the above dispersion curves, the subsurface structure beneath the site can be estimated. The PSO is a solution method for a non-linear optimization problem. We estimate the subsurface structure of the model by minimizing the difference between the observed and theoretical phase velocity curves (Kiyono et al, 2011).

$$F = \sum_{i=1}^{N} w_i \sqrt{\left(c_i^0\right)^2 - \left(c_i^T\right)^2} \qquad (1)$$

where F is an objective function that should be minimized, c_i^0 and c_i^T are the observed and theoretical phase velocities, and w_i is a weighting function. c_i^0 and c_i^T are given in discretized
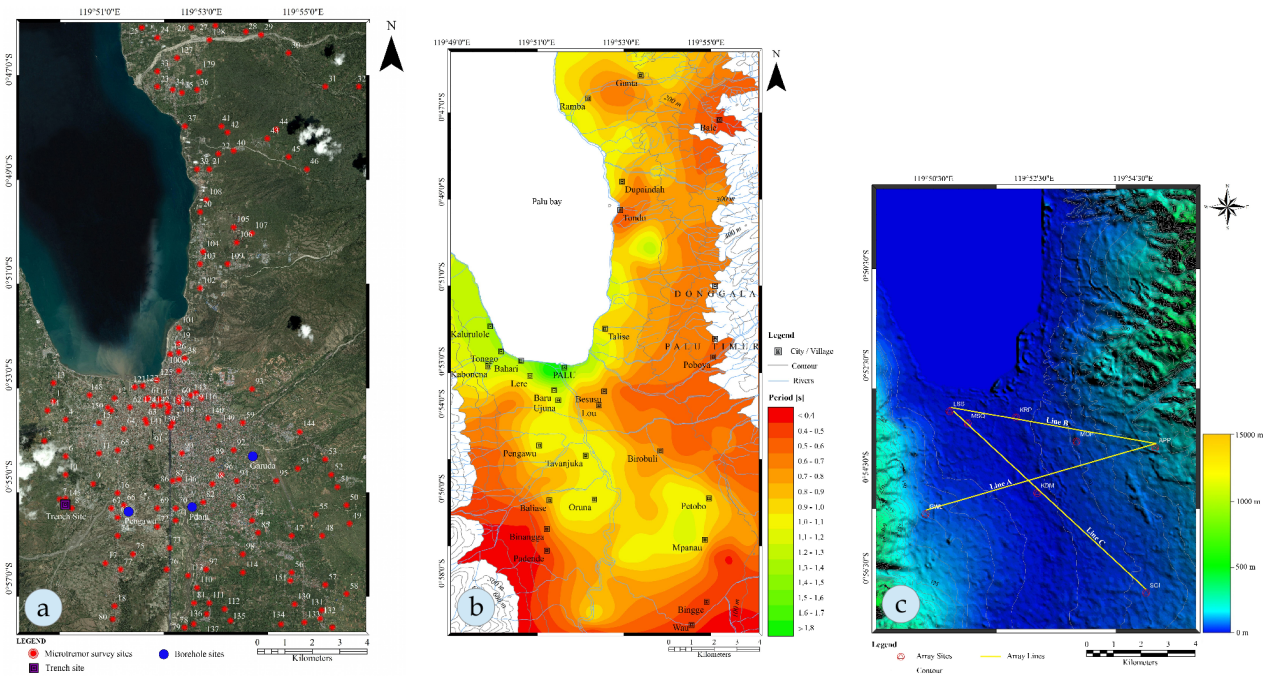
Figure 3: (a) Location of the mitcrotremor observation, boreholes sites and the situation of the trench making at Palu City; (b) Spatial distributions of longer predominant period; (c) Three survey lines for array observation (Line A, Line B, and Line C).
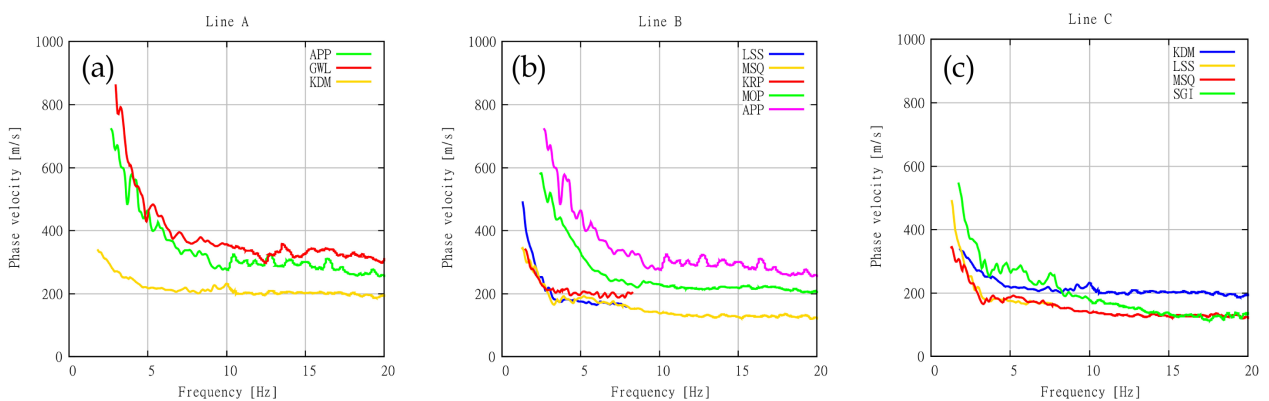

Figure 4: Dispersion curves obtained for each survey line (a) Line A, (b) Line B and (c) Line C.

frequency ($i = 1, 2, \ldots, N$). The PSO uses a particle swarm that has information about position and velocity. The particle swarm moves around the space with updating information and settles at the optimized point. During the optimization, the particle swarm has a best solution for both the group (g-best) and individual (p-best) in every step. The basic procedure of PSO is as follows. After setting the initial values of the number of particles and iterations, an initial position and velocity are given to x_d^k and v_d^k, in which d is a particle number. The value of the objective function is calculated for each particle. The best solutions for the particle, d, and for the group, g, at k-th iteration are defined as p_d^k and p_g^k. The the position and velocity are updated as

$$v_d^{k+1} = wv_d^k + c_1 r_1 \left(p_d^k - x_d^k \right) + c_2 r_2 \left(p_g^k - x_d^k \right) \tag{2}$$

$$x_d^{k+1} = x_d^k + v_d^{k+1} \tag{3}$$

where r_1 and r_2 are random values with the range of [0,1], c_1 and c_2 are constants, and w is the inertia weighting. This process is repeated as $k = k + 1$ until the number of iterations exceed a setting value. Before performing the inversion analysis, the subsurface structure was assumed to consist of horizontal layers of elastic and homogeneous medium a semi-infinite elastic body. The shear wave velocity and thickness of each layer are the parameters that were determined by inversion analysis. The results obtained enable us to determine the soil condition of the subsurface structure. Figure 5 shows V_s structures of the ground along the survey lines (a) Line A, (b) Line B and (c) Line C.

7.2 Inversion

The identified soil parameters by the inversion at MSQ and GWL are shown in Table 1 and 2. Figure 6 show dispersion curves of the ground along the survey lines at MSQ and (b) GWL, respectively.

Table 1: Identified ground parameters at MSQ.

Layer	ρ [t/m^3]	V_p [m/s]	V_s [m/s]	H [m]
1	1.7	798	124	22
2	1.8	1303	319	66
3	1.9	1496	413	198

Table 2: Identified ground parameters at GWL.

Layer	ρ [t/m^3]	V_p [m/s]	V_s [m/s]	H [m]
1	1.7	1338	335	10
2	1.8	1361	346	26
3	1.9	1814	588	63

8 Modeling of subsurface soil structure

We could obtain V_s structures at array observation sites, however, the ground profiles are not uniquely determined. In this study, we proposed simple two layer model in Palu by averaging the first three layers of all array sites. Shear wave velocity of the first layer modeled is 300m/sec. By combining with the first peak of H/V data, we can obtain the thickness of the first layer. The technique used was the 1/4 wavelength principle, which can approximately be extended to multi layered media.

$$T = 4H/V_s \tag{4}$$

where, H is a thickness of a layer, Vs shear wave velocity and T predominant period. The distribution of thickness for the first layer of which V_s is ≤ 300 m/s in Palu area is shown in Figure 7, in which the rapidly varying area of the subsurface condition and dense observation area are enclosed. The shear wave velocities, V_s^* of layers are calculated by the weighted average, for which the weight is the reciprocal of square of distance from the array observation points, APP, GWL, KDM, LSS, MOP, MSQ and SGI, as

$$V_s^* = \frac{\sum \dfrac{V_{s_i}}{x_i^2}}{\sum \dfrac{1}{x_i^2}} \tag{5}$$

where, i defines the array sites ($i = 1, 2, \ldots$ 7),and x_i indicates the distance between an array observation site and the center of the mesh.
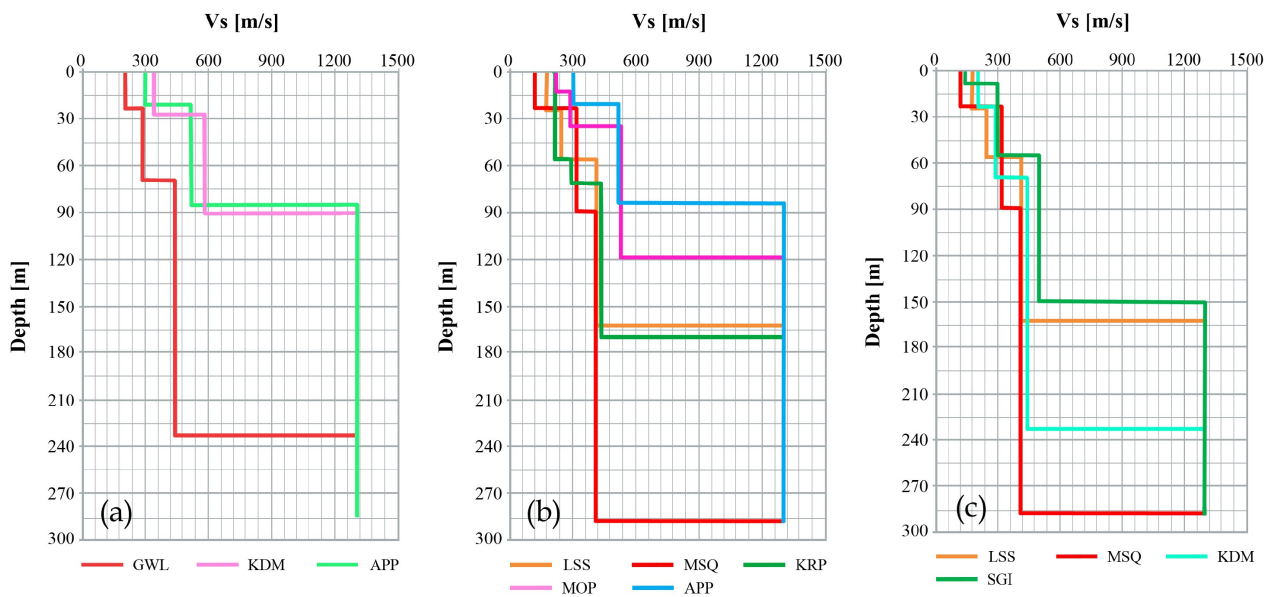
Figure 5: V_s structures of the ground along the survey lines (a) Line A, (b) Line B and (c) Line C.
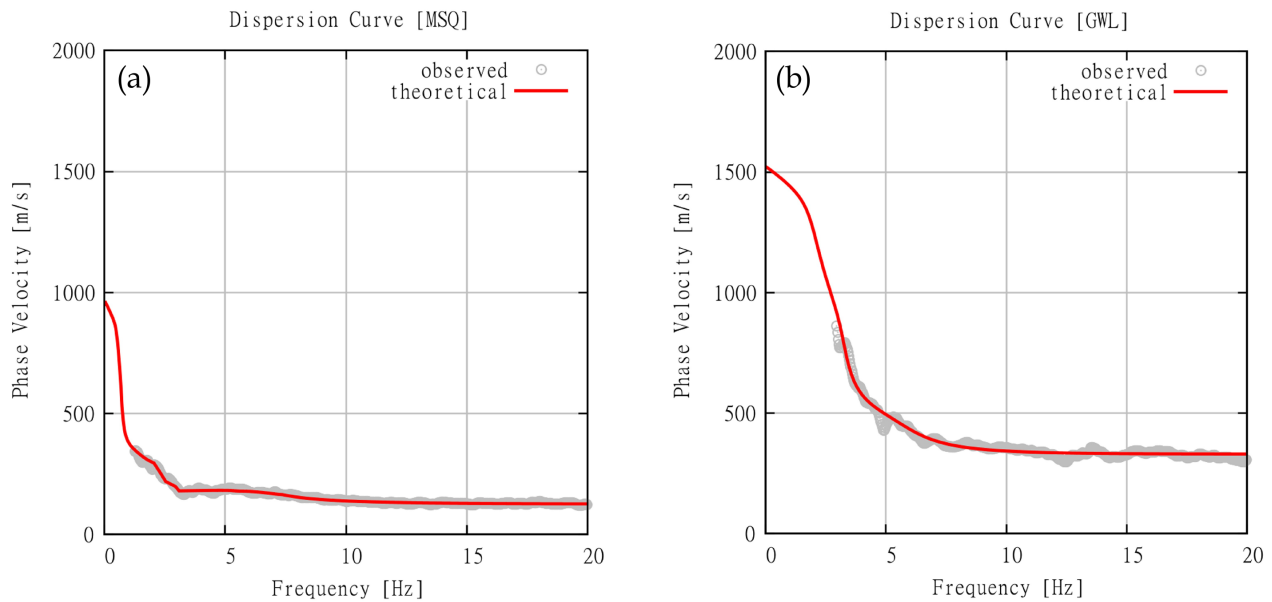

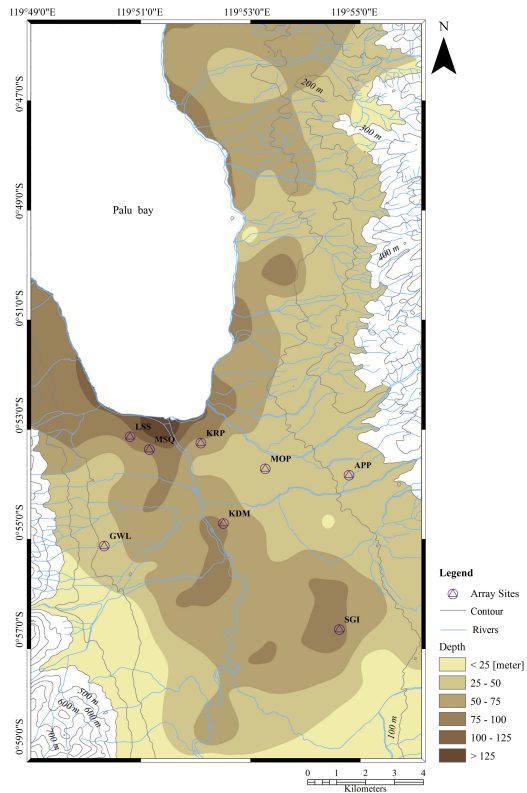Figure 6: Dispersion curves at (a) MSQ and (b) GWL.

Figure 7: Depth of the engineering bed rock.

9 Evaluation of subsurface soil profiles from boreholes

The subsurface soil profiles and related geotechnical parameters have been evaluated in three sites for determination strong ground motion and ground response analyses. The detailed drilling program had been carried out for subsurface investigation in Palu basin. There are three boreholes throughout the basin especially in Palu area to evaluate the geotechnical properties of subsurface soil layers (Figure 3). The boreholes were generally drilled up to the bedrock. The subsurface soil profiles and soil types are determined according to United State Soil Classification (USCS) system, based on grained size analysis, Atterberg's Limits Test and drill logs. The evaluated subsurface profiles for each area in the basin are shown in the following figures 8a–b.
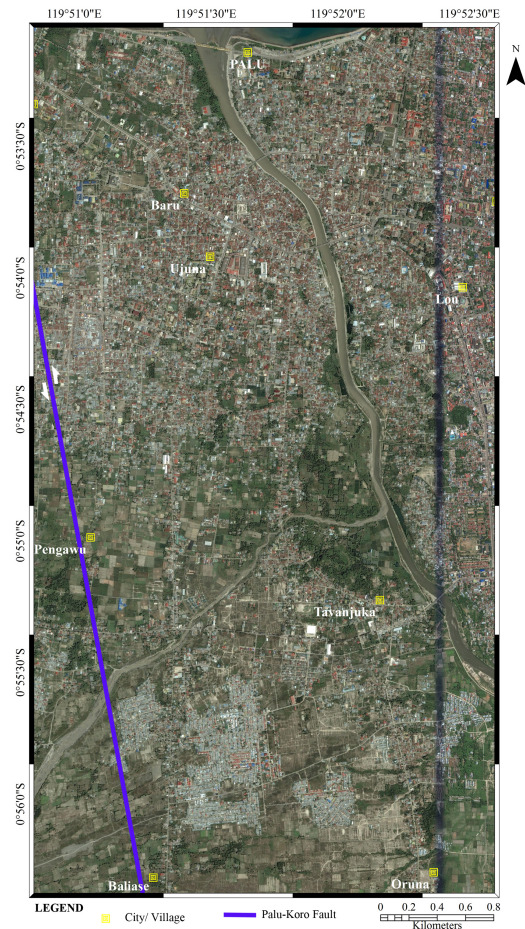

Figure 9: Location map of the Palu-Koro fault.

10 Stochastic strong ground motion simulations

Strong ground motions of the Palu area were predicted based on the stochastic green's function method (Irikura *et al.*, 2004). In this study, ground model is constructed by combining two layer model and average seismic bed rock model used in Japan, because there is no bed rock information in this area (Table 3). The fault model referred is an earthquake with moment magnitude of 6.3 on 23 January 2005 in Palu, Indonesia, of which epicenter was latitude 119.933 °E and longitude -1.198 °S. Figure 9 shows location map of the Palu-Koro fault.

10.1 Peak ground acceleration and velocity

Peak Ground Acceleration, PGA, is commonly used to describe ground motion because of their natural relationship to inertial force induced in
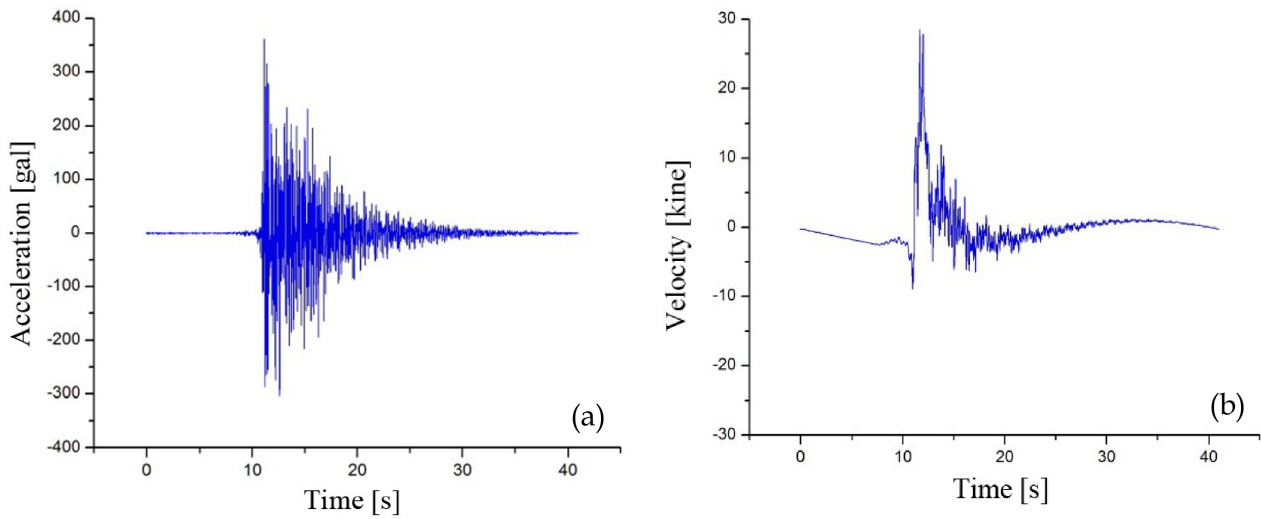
Figure 8: Soil Profiles of (a) Garuda and (b) Pengawu.

Table 3: Macroscopic source parameters

Latitude	119.933 °E	Moment magnitude	Mw = 6.3
Longitude	-1.198 °S	Fault area (km^2)	800
Top depth (d, km)	0	Shear wave velocity (km/s)	3
Bottom depth (km)	20	Mean density (ρ, t/m^3)	2.4
Length (L, km)	40	Modulus of rigidity (μ, N/m^2)	2.1E+10
Width (W, km)	20	Average slip (m)	0.21
Strike (°)	342.1	Rupture velocity (V_r, km/s)	3
Slope (°)	90	High-frequency limit (Hz)	10
Slip angle (°)	0		

certain types of structures are closely related to it. Based on acceleration histories of response analysis, PGA values are determined. The following Figure 10 (a) acceleration and (b) show and velocity time histories of APP sites. Distribution of the estimated peak ground accelerations and peak ground velocities are shown in Figure 11a and 11b. The component of the shaking is NS. There are high accelerations and velocities are as appears along the fault, especially near the epicenter. There occurred relatively large shaking at the mouth of Palu river because of the deeper thickness of the sediment. Peak acceleration becomes more than 0.40 g in some areas, which causes severe damage for buildings in high probability. To prevent severe damage, firstly we have to check the vulnerability of the building in Palu, and if necessary, we have to take a countermeasure for strengthening of the structures. This is the first trial to estimate the shaking and the damage under the condition of the occurrence of a future Palu-Koro earthquake. We accumulate detailed information about not only the ground but also the inventory for disaster mitigation in Palu.

10.2 Ground shear strain

This research is to establish a simplified accurate method to evaluate the ground shear strain and vulnerability of the ground structures using microtremor. The vulnerability index is expected to be generalized as compared with actual earthquake damage. When shear deformation at ground surface at the time of earthquake is set to δg, the strain of surface ground γg is expressed as follows in approximation:

$$
\begin{aligned}
\gamma_g &= \delta_g/h \\
&= e \times a/\left(2\pi F_g\right)^2 \times 4F_g/v_s \\
&= e \times A_g \times a/\left(\pi^2 F_g v_b\right)^2 \times v_b/v_s \quad (6) \\
&= \left(\frac{A_g^2}{F_g}\right) \times \left(\frac{e \times a}{\pi^2 \times v_b}\right)
\end{aligned}
$$

$$
\gamma_g = K_g \times C \times a \quad (7)
$$

where,

$$
\begin{aligned}
K_g &= A_g^2/F_g \\
C &= e/2 \cdot v_b
\end{aligned} \quad (8)
$$

γ_g : shear strain (in powers of 10^{-6}); A_g : amplification factor of the surface ground $(= v_b/v_s)$; F_g : natural frequency of the surface ground $(\mathrm{Hz})(= v_s/4h)$; a : maximum acceleration of the basement (Gal); e : efficiency of the maximum acceleration; v_b : S-wave velocity of the basement (m/s); v_s : S-wave velocity of surface ground (m/s); h: thickness of surface ground.

Here, if it is assumed that it is $v_b \leq 1300$ m/s and $e = 0.6$, it is come to C = 1.0. Effective strain can be presumed as a value which multiplied by K_g value and the maximum acceleration in case of an earthquake. K_g value is an index peculiar to the measured ground, and it is possible to express the vulnerability of the ground. As shown in equation (8), K_g value can be easily derived from natural frequency F_g and amplification factor A_g which were presumed in each measurement point. Figure 11c shows the ground shear strain map of Palu City.

11 Conclusions

The procedure employed and conclusions obtained in this study are as follows. Microtremor observations were carried out for constructing a subsurface ground model in Palu City. Single-point observations and array observations were conducted at 151 and 8 sites respectively, which covered almost the whole city area. The subsurface structure investigation had been performed by boring survey at three selected sites; Garuda, Pengawu and PDAM. Based on drill core data and SPT results, the simplified subsurface soil layers were evaluated. H/V spectra were calculated at all the single observation sites and a distribution of predominant periods was obtained. The dispersion curves of a Rayleigh wave were obtained from the data of array observations. By conducting an inversion analysis for the calculation of dispersion curves, the subsurface structure beneath the site can be estimated. It was constructed a four layered model in each array observation point. This research was reconstructed unified two-layered model by averaging the first three layers obtained from array observation. The shear wave velocity of the top layer is $V_s \leq 300$ m/s.
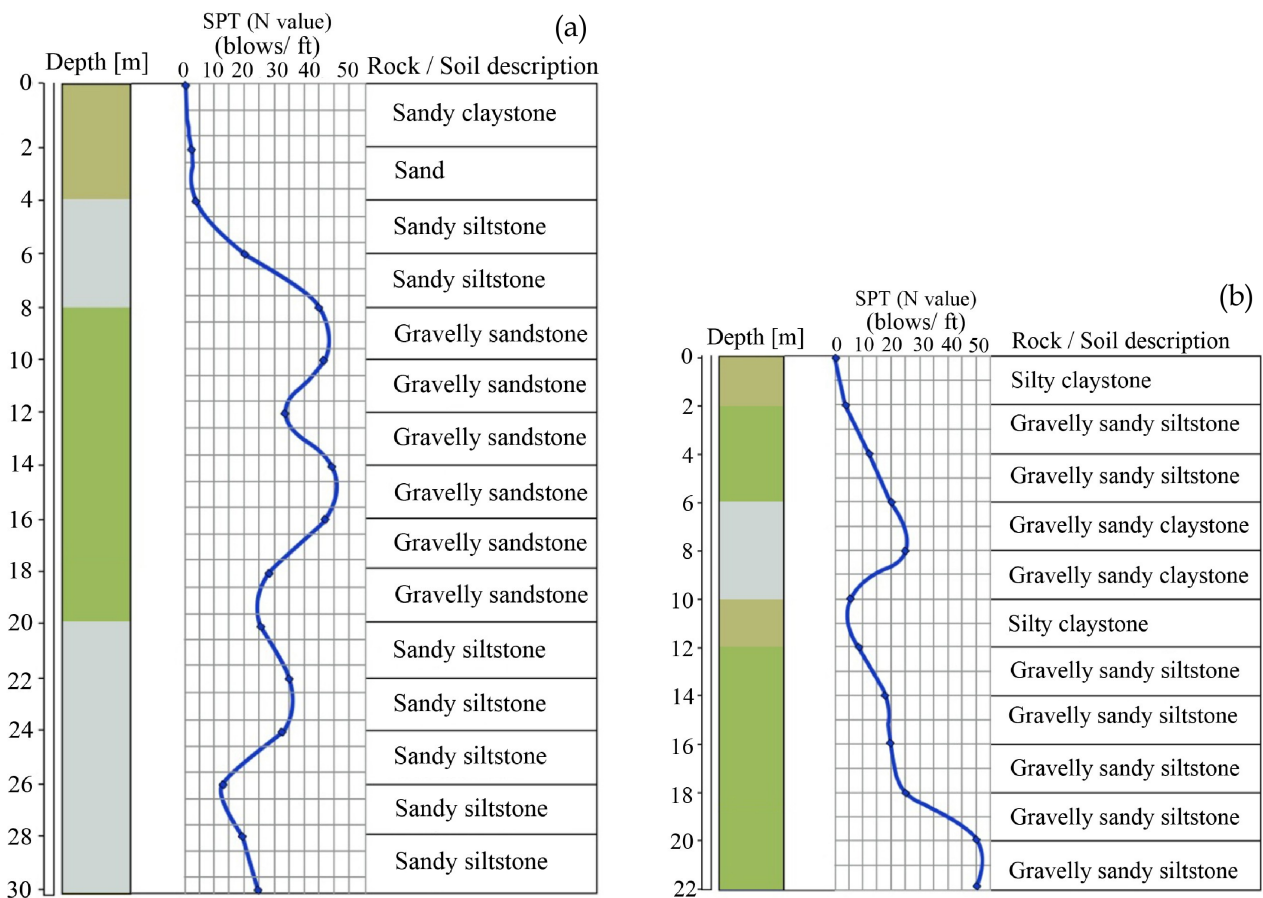
Figure 10: (a) Palu earthquake peak ground acceleration (North-South direction), and (b) peak ground velocity (Up-Down direction) record of APP site.
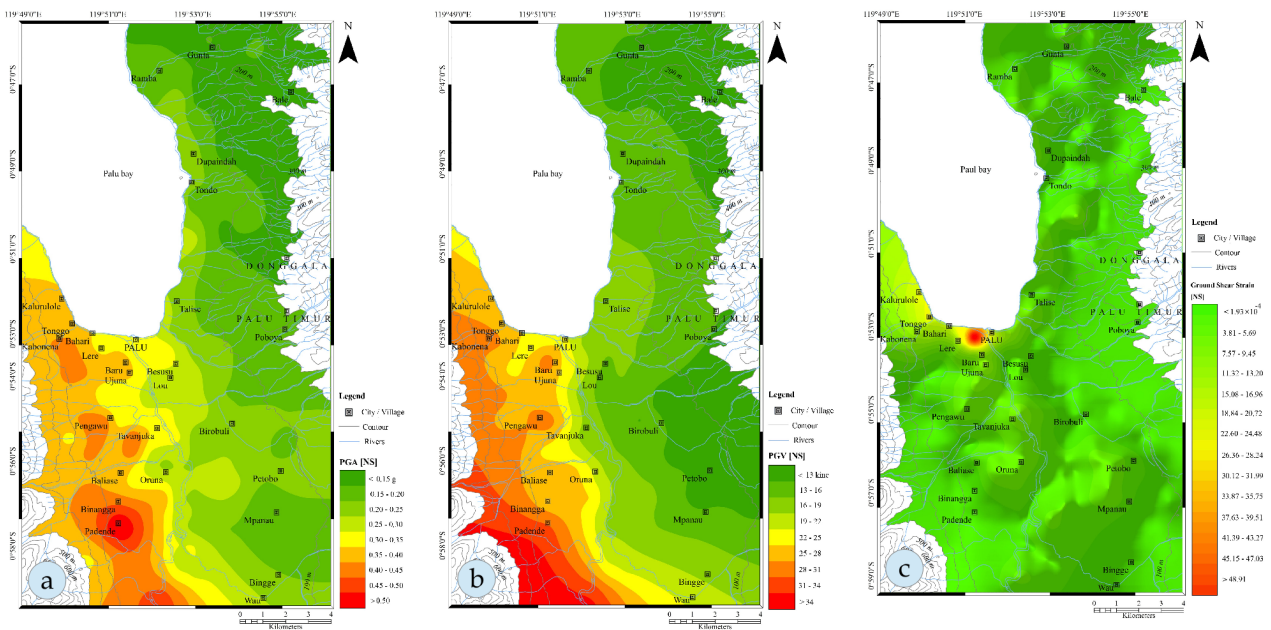

Figure 11: (a) Peak ground acceleration [NS] map on Palu area; (b) Peak ground velocity [NS] map on Palu area; (c) Map of Ground Shear Strain (NS) in Palu City.

Three dimensional structure for shear wave velocities were (I) $V_s \leq 300$ m/s, (II) $300\text{m/s} \leq V_s \geq 1300$ m/s and (III) $V_s \geq 3000$ m/s. By combining above two-layer model and the results of single point observation, the distribution of the first layer thickness of the sediment is obtained. The Kriging method can be used for the interpolation of subsurface information such as predominant period, shear wave velocity and depth of irregular boundary. Palu City had deposited on a thick alluvial layer in the coastal area (with a sedimentary layers between 75 and greater than 125 m) that thins toward the mountains (with a sedimentary layers less than 25 m). The subsurface geology also changes slowly from soft sedimentary layers in the coastal area to igneous intrusion and metamorphic rock in the mountains. The resulted PGA and PGV maps show that some severe damaged areas during January 23, 2005 earthquake is related to strong ground motion and some are related to high amplification of local sediments. Microtremor survey results showed that in hilly areas had low ground shear strain index, whereas in coastal alluvium was composed of material having a high ground shear strain indication.

Acknowledgements

References

Aki, K. (1957) Space and time spectra of stationary stochastic waves, with special reference to microtremor, Bull. Earth. Res. Inst., vol. 35(3), pp. 415–456.

Ananda, S. R. (2013) Analisis dan Interpretasi Kelurusan Struktur Geologi Menggunakan Digital Elevation Model (DEM) ASTER Daerah Kecamatan Palu Timur dan Sigibiromaru, Kabupaten Donggala, Kota Palu, Gadjah Mada University, 2013.

Indra, I. I. A. (2013) Analisis dan Interpretasi Struktur Geologi Menggunakan Digital Elevation Model (DEM) ASTER Daerah Kecamatan Marawola, Dolo, dan Palu Barat, Kota Palu, Sulawesi Tengah, Gadjah Mada University, 2013.

Irikura, K., Miyake, H., Iwata, T., Kamae, K., Kawabe, H. and Dalguer, L. A (2004) Recipe for predicting strong ground motion from future large earthquake, Proceedings of the 13th World Conference on Earthquake Engineering, No. 1371.

Ismawan, G.F. (2013) Geologi dan Analisis Struktur Geologi Berdasarkan Digital Elevation Model (DEM) ASTER Daerah Palu Barat dan Marawola, Kota Palu, Poopinsi Sulawesi Tengah, Gadjah Mada University, 2013.

Juwanto, D. (2013) Studi Struktur Geologi Tepi Timur Lembah Palu Kecamatan Palu Timut, dan Tavaili, Kota Palu, Gadjah Mada University, 2013.

Keneddy, J. and Eberhart. R.C. (1995) Particle swarm optimization, Proc. of IEEE. International conference on Neural Networks, Vol.4, pp.1942-1948.

Kiyono, J. and Suzuki, M. (1996) Conditional Simulation of Stochastic Waves by Using Kalman Filter and Kriging Techniques, Proc. of the 11th World Conference on Earthquake Engineering, Acapulco, Mexico, No.1620.

Kiyono, J., Ono, Y., Sato, A., Noguchi, T. and Rusnardi, P.R. (2011) Estimation of subsurface structure based on Microtremor observations at Padang, Indonesia, ASEAN Engineering Journal, Vol.1, No.3, pp.66-81.

Noguchi, T., Horio, T., Kubo, M., Ono,Y., Kiyono, J., Ikeda, T. and Rusnardi, R.P. (2009) Estimation of Subsurface Structure in Padang, Indonesia by Using Microtremor Observation, Report on Earthquake Disaster Prevention Field, Tono Research Institute of

Earthquake Science, Seq. No.26, pp.1-16, (in Japanese)

Pramumijoyo, S., Indarto, S., Widiwijayanti, C., and Sopaheluwakan, J. (1997) Seismic Parameters of the Palu-Koro Fault in Palu Depression Area, Central Sulawesi. Indonesia J. SE Asian Earth Sci.

Priadi, B. (1993) Geochimie du magmatisme de l'Ouestet du Nord de Sulawesi, Indonesia:Tracage des sources et implications geodynamique. Doctoral thesis, Universite Paul Sabatier, Toulouse, France.

Soekamto, R.A.B. (1995) Regional Geological Map of Palu Sheet, Indonesia, Scale 1:250,000, Geological Research Center, Bandung.

Thein, P.S., Pramumijoyo, S., Brotopuspito, K.S., Wilopo, W., Kiyono, J and Setianto, A. (2013) Site response characteristics of H/V spectrum by microtremor single station observations at Palu City, Indonesia. Journal of Southeast Asian Applied Geology, Volume 5, Number 1, January-June 2013. ISBN 2086-5104. USGS, (2007), Historical World wide Earthquake (http://earthquake.usgs.gov/).